Development 137, 1595-1599 (2010) doi:10.1242/dev.046888

Emergence of traveling waves in the zebrafish segmentation clock

Kana Ishimatsu[1], Atsuko Takamatsu[2] and Hiroyuki Takeda[1,*]

SUMMARY

The spatial and temporal periodicity of somite formation is controlled by the segmentation clock, in which numerous cells cyclically express *hairy*-related transcriptional repressors with a posterior-to-anterior phase delay, creating 'traveling waves' of *her1* expression. In zebrafish, the first traveling wave buds off from the synchronous oscillation zone in the blastoderm margin. Here we show that the emergence of a traveling wave coincides with the anterior expansion of Fgf signaling and that transplanted Fgf8b-soaked beads induce ectopic traveling waves. We thus propose that as development proceeds, the activity of Fgf signaling gradually expands anteriorly, starting from the margin, so that cells initiate *her1* oscillation with a posterior-to-anterior phase delay. Furthermore, we suggest that Fgf has an essential role in establishing the period gradient that is required for the *her1* spatial oscillation pattern at the emergence of the traveling wave.

KEY WORDS: Fgf, *her1*, Oscillation, Segmentation clock, Traveling waves, Zebrafish

INTRODUCTION

The periodic formation of vertebrate somites is governed by the segmentation clock, a congregation of cells that exhibit oscillating expression of *hairy*-related transcriptional repressors (*her1* and *her7* in zebrafish) through a negative-feedback loop. In zebrafish, a somite is formed every 30 minutes, and the segmentation clock cyclically exhibits a dynamic spatial pattern of *hairy* gene expression in the presomitic mesoderm (PSM) with the same periodicity (Fig. 1A, left). Previous reports have demonstrated that the phases of cellular oscillation are highly coordinated in a spatial manner, which results in traveling waves that repeatedly bud off from the synchronized oscillation zone in the posterior PSM, sweep anteriorly, and stop around the future segmentation point (Fig. 1A, middle) (Gajewski et al., 2003; Henry et al., 2002; Holley et al., 2000; Holley et al., 2002; Horikawa et al., 2006; Jiang et al., 2000; Oates and Ho, 2002; Palmeirim et al., 1997; Pourquie, 2003; Saga and Takeda, 2001; Sawada et al., 2000). The traveling waves are the result of phase differences among the oscillating cells in a posterior-to-anterior direction; cells with nuclear dots, with cytoplasmic signals and with no signal are detected sequentially from anterior to posterior, corresponding to transcribing cells, translating cells and non-transcribing cells, respectively (Fig. 1A, right). This pattern of oscillation is maintained throughout segmentation and is referred to as the 'mature' pattern. Although many studies have addressed the mechanisms of the mature segmentation clock, very few investigations have focused on the initiation of the segmentation clock (Riedel-Kruse et al., 2007) and little is known about how the traveling wave emerges. In the present study, we investigate this early mechanism through in vivo and in silico experiments using zebrafish as a model system.

[1]Department of Biological Sciences, Graduate School of Science, University of Tokyo, Hongo 7-3-1, Tokyo 113-0033, Japan. [2]Department of Electrical Engineering and Bioscience, Waseda University, 3-4-1 Okubo, Shinjuku-ku, Tokyo 169-8555, Japan.

*Author for correspondence (htakeda@biol.s.u-tokyo.ac.jp)

Accepted 3 March 2010

MATERIALS AND METHODS

In situ hybridization

Whole-mount in situ hybridization (Nikaido et al., 1997) and fluorescent in situ hybridization (Horikawa et al., 2006) were performed as previously described.

Fgf bead transplantation and SU5402 treatment

Fgf8b-soaked bead transplantation and SU5402 treatment were performed as described (Sawada et al., 2001). Bead transplantation was performed at the 30% epiboly stage (~5.0 hpf, as indicated in Fig. S1A in the supplementary material). SU5402 (Calbiochem) treatment was performed at 0.2 mg/ml for 8 minutes (strong treatment in Fig. 2B) or 4 minutes (weak inhibition in Fig. 3A). Then, the embryos were incubated in Ringer's solution for 2 hours.

Time-lapse imaging

Embryos transplanted with Alexa488-injected cells were mounted in 1% agarose. Images were collected at 10-minute intervals with a MZFLIII fluorescence microscope (Leica). Cell tracking and quantification were performed with ImageJ (NIH).

Morpholino injection

Antisense morpholino oligonucleotides for *her1/7* were designed as described previously (Henry et al., 2002). Morpholinos were injected at 0.25 mM into single-cell stage embryos.

RESULTS AND DISCUSSION

Emergence of the traveling waves

The traveling wave in an anterior direction first appears at ~70% epiboly [7.8 hours post-fertilization (hpf)], long (~3 hours) before segmentation takes place (Fig. 1B-E; see Fig. S1A in the supplementary material) (Riedel-Kruse et al., 2007). Until this point, *her1* oscillation is restricted to the blastoderm margin and is synchronized among cells in this area as reported previously (Riedel-Kruse et al., 2007). At the initiation of the traveling wave, phase delay in an anterior direction is observed, indicating that the traveling wave is created mainly by sequential initiation of *her1* oscillation from posterior to anterior. During the synchronous oscillation in the margin, gastrulation movement towards the anterior occurs (see Fig. S1B in the supplementary material) (Warga

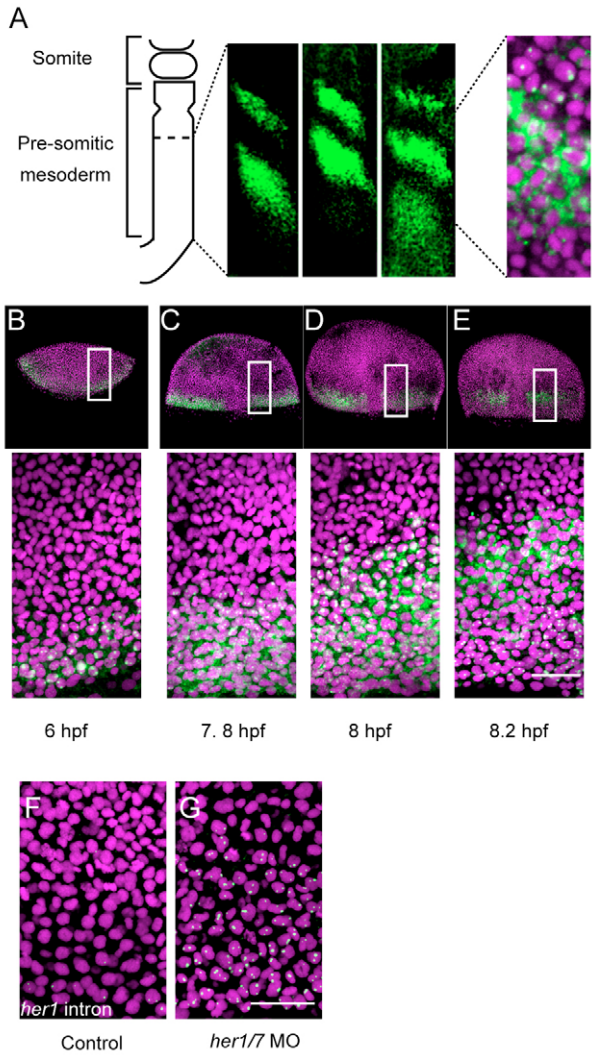

Fig. 1. Overview of the segmentation clock in the zebrafish embryo. Anterior to top, posterior to bottom. Green, *her1* mRNA in situ hybridization; magenta, nuclear counterstain. (**A**) Subcellular localization of *her1* mRNA in the traveling wave during the segmentation stage. (**B-E**) Emergence of the traveling wave at the blastula stage. The boxed regions are enlarged in the panels beneath. (**F**,**G**) Control and *her1/7* morpholino-injected samples. The injected morpholino was designed against the first ATG and *her1* transcripts were detected with the intron probe; thus, the signals detected cannot result from mRNA stabilized by morpholino binding. Scale bar: 50 μm.

and Kimmel, 1990), indicating that the marginal cells, which transiently expressed *her1*, attain a transcription-negative state when the cells exit the marginal area and form the hypoblast layer. This was further supported by a comparison between expression of the PSM marker *papc* (*pcdh8* – Zebrafish Information Network) and *her1* (see Fig. S1B in the supplementary material). *her1/7* morpholino injection also revealed that the suppression of *her1* in the hypoblast depends on its own negative feedback: the *her1* expression domain was found to be broadened in morpholino-injected embryos, whereas it was restricted to the marginal area in control embryos (7.0 hpf) (Fig. 1F,G). We did not observe the horizontal waves from ventral to dorsal previously reported (Riedel-Kruse et al., 2007), although we performed precise time-course analysis of *her1* expression using embryos of strictly controlled stages (see Fig. S1A in the supplementary material). In the following experiments we focus on the mechanism underlying the emergence of the first traveling wave.

Fgf signaling triggers *her1* oscillation and formation of the traveling wave

Intercellular communication through the Notch pathway is dispensable for the initiation of traveling waves as revealed both by Notch mutants (Jiang et al., 2000) and inhibitor experiments (see Fig. S2A-C in the supplementary material). Furthermore, other types of communication might not be required as our preliminary data suggest that wild-type cells initiate *her1* expression when they are surrounded by non-oscillating mutant cells (see Fig. S2D,E in the supplementary material). It is also unlikely that the anterior movement of the mesoderm plays any role, as it would result only in a phase advance towards the anterior and not in a phase delay. These facts led us to speculate that the traveling wave is generated by an extracellular factor that triggers *her1* oscillation. Previous studies have shown that Fgf signaling is necessary for clock oscillation in mouse and that Fgf actually induces *Hes1* oscillation in murine cultured cells (Nakayama et al., 2008; Niwa et al., 2007; Wahl et al., 2007). Fgf signaling is also known to control the spatial pattern of *hairy* gene oscillation in zebrafish and chick (Dubrulle et al., 2001; Sawada et al., 2001). However, the role of Fgf in initiating the traveling wave has not been studied. We therefore examined its role in the emergence of the traveling wave in zebrafish embryos.

We found that *fgf8a* is expressed at the expected stages and location (Fig. 2A). We first confirmed in zebrafish that Fgf is necessary for *her1* expression. Treatment of whole embryos with SU5402, a chemical inhibitor of Fgf signaling, abolished the intrinsic traveling waves as well as the marginal *her1* oscillation at early stages (Fig. 2B), consistent with previous findings in mouse (Niwa et al., 2007; Wahl et al., 2007). We then asked whether ectopic activation of Fgf signaling would induce *her1* oscillation in the embryo. We transplanted Fgf8b-soaked beads into embryos at the stage before the emergence of the traveling wave (see Fig. 2C for ectopic Fgf activity), and then examined their effect on *her1* expression 0.5-1.5 hours after transplantation. The results were striking in that the ectopic *her1* expression gradually expanded with time, forming a band of *her1* expression around the bead in 9 out of 22 dorsally transplanted samples (Fig. 2D), whereas the remainder exhibited ectopic non-band-like expression of *her1* around the beads. We confirmed that this ectopic *her1* stripe was actually a traveling wave by observing a spatial transcriptional delay in the direction away from the bead: the cells at the transcription-negative, translational and transcriptional states were detected in sequence starting from the site of bead transplantation (Fig. 2E,F). The induced traveling waves were however restricted to the dorsal side and to the mesodermal layer, forming an incomplete circle (Fig. 2G). This suggests the presence of other permissive factors for *her1* expression in the future PSM, before the endogenous wave emerges.

One possible mechanism for creating traveling waves by Fgf signaling is that Fgf activity gradually expands in the anterior direction so that it induces *her1* oscillation in sequence with a phase delay. To monitor the activity of Fgf signaling, we examined the expression of *sprouty 4* (*spry4*), one of the well-known downstream genes of Fgf signaling, and found that Fgf activity indeed gradually expands anteriorly from the restricted region of the margin (Fig. 2H; see Fig. S1B in the supplementary material). The timing of *spry4* expansion correlated well with the emergence of the first traveling wave (Fig. 2H-J; see Fig. S1B in the supplementary material). The

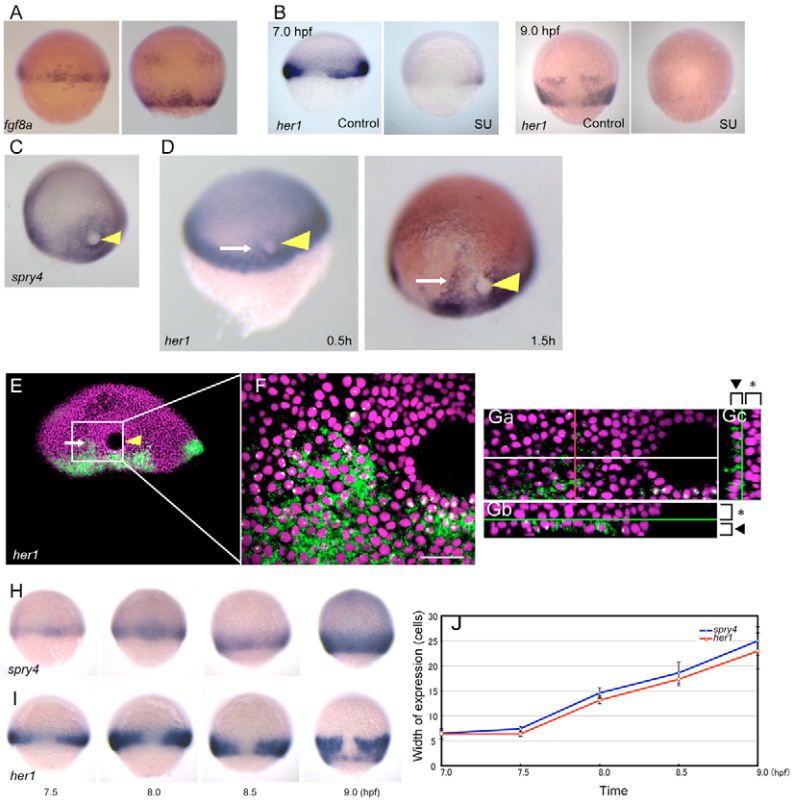

Fig. 2. *her1* oscillation is induced by Fgf. (**A**) Expression of *fgf8a* at the mid (left) and late (right) epiboly stage. (**B**) *her1* expression disappears following treatment with the Fgf inhibitor SU5402. Left and right panels show *her1* expression at the stage before (7.0 hpf) and after (9.0 hpf) the emergence of the traveling wave, respectively. (**C-G**) Ectopic Fgf induces an ectopic *her1* traveling wave. (C) Ectopic expression of *spry4* was induced by Fgf8b-soaked bead implantation (arrowhead). (D) Ectopic *her1* expression (arrow) is first detected in close vicinity to the Fgf bead (left, 0.5 hours after transplantation) and tends to gradually expand with time, forming a band-like expression domain (right, 1.5 hours after transplantation). (E,F) Subcellular localization of induced *her1* expression. (Ga-c) Induction of the traveling wave by Fgf bead transplantation occurs only in the hypoblast. Optical sections of the sample shown in E,F along the *z*-axis (Ga), *x*-axis (Gb) and *y*-axis (Gc). *x*- and *y*-axes are shown by white and red lines, respectively, in Ga. Hypoblast and epiblast are indicated by arrowheads and asterisks, respectively. (**H**,**I**) The regions of Fgf activity, as indicated by *spry4* (H), and *her1* expression (I) are almost identical. (**J**) Time-course analysis of the width (in cells) of *spry4* and *her1* expression. The number of cells showing nuclear signals was manually counted in samples subjected to high-resolution in situ hybridization (images not shown). Error bars indicate s.d. Scale bar: 50 μm.

mechanism that expands Fgf activity at this stage remains elusive, although endocytosis could regulate this process (Scholpp and Brand, 2004). Taken together, we conclude that the anterior expansion of Fgf activity triggers the first traveling wave that leaves the marginal expression domain.

Fgf signaling is responsible for the period gradient of the traveling wave

In the mature segmentation clock, the stripes of *her1* become narrower as they move anteriorly. This characteristic oscillation pattern has been considered to result from a gradient in the oscillation period along the anterior-posterior (AP) axis (Giudicelli et al., 2007; Gomez et al., 2008; Morelli et al., 2009; Palmeirim et al., 1997; Uriu et al., 2009), which is shorter in the posterior and longer in the anterior PSM. We also confirmed this idea using the phase oscillator model (see Fig. S3 in the supplementary material). This idea appears to hold true at the emergence of the traveling wave because the first traveling wave also becomes narrower as it moves. Furthermore, the Fgf activity gradient (higher in the posterior PSM) is known to affect the spatial oscillation pattern of *her1* (Dubrulle et al., 2001; Sawada et al., 2001). These facts raise the possibility that early Fgf signaling regulates the period, as well as the timing of initiation, of *her1* oscillation at the emergence of the traveling wave. To directly test this possibility, we weakly inhibited gastrulating embryos with SU5402, in which the gradient of Fgf activity was expected to be uniformly decreased. When the stripe first appeared (for control, t=60; for SU5402 treated, t=90), the *her1* stripe in treated embryos became narrower and was formed at a more posterior site than that in control embryos (Fig. 3A). Under our experimental conditions, the mesoderm was maintained after SU5402 treatment, but the PSM was reduced in size along the AP axis (see Fig. S4A in the supplementary material). The reduction in PSM size, however, might not account for the narrower and posteriorly shifted *her1* expression band in SU5402-treated embryos because the *her1* expression pattern is thought to depend primarily on the oscillation dynamics of unit oscillators (e.g. the period) (Giudicelli et al., 2007; Gomez et al., 2008; Morelli et al., 2009; Palmeirim et al., 1997; Uriu et al., 2009). Furthermore, the effect of SU5402 treatment on cellular movement was limited (Fig. 3B; see Fig. S4B in the supplementary material). Taken together, we conclude that the observed change in *her1* stripes induced by SU5402 treatment was mainly attributable to the altered dynamics of *her1* oscillation.

Since we were unable to determine directly whether the results obtained by SU5402 treatment were the consequence of an altered oscillation period, we instead assessed the effect of altered period on the spatial oscillation pattern in a mathematical simulation, using the phase oscillator model (see Fig. S3 in the supplementary material). For control embryos, we set the intrinsic frequency (the frequency intrinsically given to each virtual oscillator) as the green line in Fig. 3Ca, so that the observed frequency (the actual frequency in simulation, which is not identical to the intrinsic frequency as a result of cellular coupling) also forms a similar gradient as indicated by the green line in Fig. 3Cb. This reproduced the normal emergence of traveling waves in silico (Fig. 3Cc, left). We then examined the spatial oscillation pattern when the gradient of the intrinsic frequency is uniformly decreased, a situation expected to occur when embryos are treated with SU5402 (Fig. 3Ca,b). Under this condition, the phenotype obtained in vivo is clearly reproduced in the simulation, resulting in a posteriorly shifted and narrower stripe (Fig. 3Cc, right). Furthermore, the opposite phenotype was obtained with Fgf bead transplantation (see Fig. S5 in the supplementary material). All these data support the idea that the oscillation period is controlled by Fgf signaling.

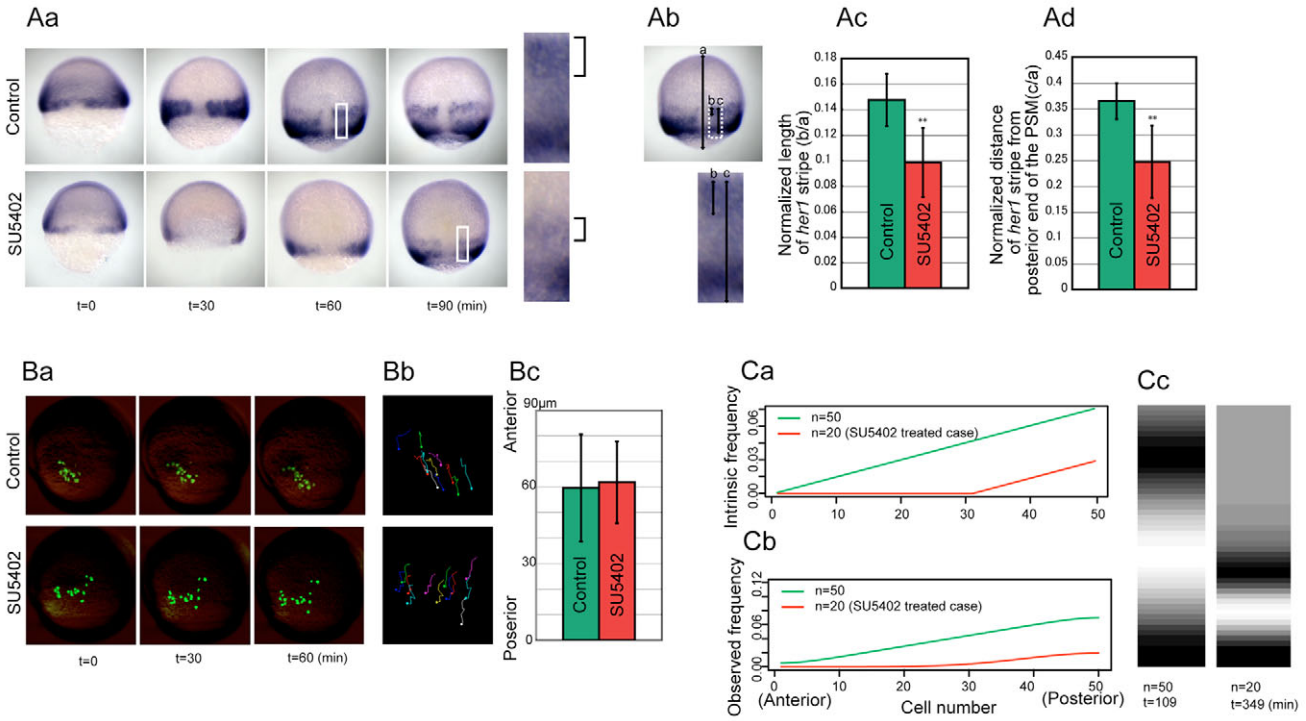

Fig. 3. Effect of Fgf inhibition on the *her1* oscillation period. (**Aa-d**) Effect of compromised Fgf signaling on the spatial oscillation pattern of *her1*. (a) Time series of *her1* expression in control (upper) and SU5402-treated (lower) zebrafish embryos. We set the 50% epiboly stage as *t*=0. The boxed regions, in those images taken at the time points that the *her1* stripe first appears, are enlarged to the right. Brackets indicate the first *her1* stripes. (b) The length of the *her1* stripe (line b) and the distance between the *her1* stripe and the posterior end of the PSM (line c) were measured and normalized by embryonic size (line a). (c,d) The normalized length of the *her1* stripe and the normalized distance of the *her1* stripe from the posterior end of the PSM in SU5402-treated embryos were significantly shorter than in the control; **, $P<0.01$ (n=12 for control embryos and n=11 for SU5402 treatment). Error bars indicate s.d. (**Ba-c**) The effect of SU5402 treatment on gastrulation cell movement was limited. (a) Time-course images of the labeled cells with or without SU5402 treatment. The cellular movement was then tracked every 10 minutes (b) and quantified (c). The mean net displacement towards the posterior direction (n=25 cells from three embryos for control and n=34 cells from three embryos for SU5402 treatment) reveals no significant difference in gastrulation movement following the treatment (c). Error bars indicate s.d. (**Ca-c**) Simulation of a decreased frequency gradient. (a,b) The intrinsic (a) and observed (b) frequency. n indicates the number of cells that were given the gradient of intrinsic frequency. The intrinsic frequency for the SU5402-treated case was fixed at 0 in the cells i=1-30 (a, red) (see Fig. S3 in the supplementary material). (c) The simulated stripe pattern of *her1* expression when the stripe first appeared in each condition. n and t beneath the panels indicate the number of cells that were given the gradient of intrinsic frequency and the elapsed time, respectively. Coupling between non-oscillatory cells (n=0-30 in the SU5402-treated case) and oscillatory cells was maintained in this simulation, but we confirmed that the same trend was obtained in the absence of coupling.

Taken together, our findings suggest that at the emergence of the traveling wave, the initiation timing and the oscillation period of *her1* are simultaneously controlled by Fgf and co-operatively establish the posterior-to-anterior phase delay in the oscillatory field. In wild-type embryos, the traveling waves appear in a highly coordinated manner despite dynamic morphogenesis during gastrulation. The global control of cellular oscillators by secreted factors, such as Fgfs, could be crucial in this situation. The mechanism by which Fgf signaling modulates *her1* negative feedback to induce *her1* oscillation and alter the *her1* oscillation period remains to be established. Further effort aimed at direct measurements of each reaction step in the *her1* negative-feedback loop in response to Fgf will help to identify the Fgf target step, and improve our current understanding of the basic principles governing the emergence of the traveling wave.

Acknowledgements
We thank Dr Sharron Amercher for providing *her1/7* deletion mutants; Dr Julian Lewis for advice and helpful discussions; and the National BioResource Project, Zebrafish, NBRP/Brain Science Institute, RIKEN for zebrafish supply. This work was supported in part by Grants-in-Aid for Scientific Research Priority Area Genome Science and Scientific Research (A and B) and Global COE Program (Integrative Life Science Based on the Study of Biosignaling Mechanisms) from the Ministry of Education, Culture, Sports, Science and Technology (MEXT) of Japan. K.I. was supported by Research Fellowships for Young Scientists from the Japan Society for the Promotion of Science.

Competing interests statement
The authors declare no competing financial interests.

Supplementary material
Supplementary material for this article is available at
http://dev.biologists.org/lookup/suppl/doi:10.1242/dev.046888/-/DC1

References

Dubrulle, J., McGrew, M. J. and Pourquie, O. (2001). FGF signaling controls somite boundary position and regulates segmentation clock control of spatiotemporal Hox gene activation. *Cell* **106**, 219-232.
Gajewski, M., Sieger, D., Alt, B., Leve, C., Hans, S., Wolff, C., Rohr, K. B. and Tautz, D. (2003). Anterior and posterior waves of cyclic her1 gene expression are differentially regulated in the presomitic mesoderm of zebrafish. *Development* **130**, 4269-4278.
Giudicelli, F., Ozbudak, E. M., Wright, G. J. and Lewis, J. (2007). Setting the tempo in development: an investigation of the zebrafish somite clock mechanism. *PLoS Biol.* **5**, e150.

Gomez, C., Ozbudak, E. M., Wunderlich, J., Baumann, D., Lewis, J. and Pourquie, O. (2008). Control of segment number in vertebrate embryos. *Nature* **454**, 335-339.
Henry, C. A., Urban, M. K., Dill, K. K., Merlie, J. P., Page, M. F., Kimmel, C. B. and Amacher, S. L. (2002). Two linked hairy/Enhancer of split-related zebrafish genes, her1 and her7, function together to refine alternating somite boundaries. *Development* **129**, 3693-3704.
Holley, S. A., Geisler, R. and Nusslein-Volhard, C. (2000). Control of her1 expression during zebrafish somitogenesis by a delta-dependent oscillator and an independent wave-front activity. *Genes Dev.* **14**, 1678-1690.
Holley, S. A., Julich, D., Rauch, G. J., Geisler, R. and Nusslein-Volhard, C. (2002). her1 and the notch pathway function within the oscillator mechanism that regulates zebrafish somitogenesis. *Development* **129**, 1175-1183.
Horikawa, K., Ishimatsu, K., Yoshimoto, E., Kondo, S. and Takeda, H. (2006). Noise-resistant and synchronized oscillation of the segmentation clock. *Nature* **441**, 719-723.
Jiang, Y. J., Aerne, B. L., Smithers, L., Haddon, C., Ish-Horowicz, D. and Lewis, J. (2000). Notch signalling and the synchronization of the somite segmentation clock. *Nature* **408**, 475-479.
Morelli, L. G., Ares, S., Herrgen, L., Schroter, C., Julicher, F. and Oates, A. C. (2009). Delayed coupling theory of vertebrate segmentation. *HFSP J.* **3**, 55-66.
Nakayama, K., Satoh, T., Igari, A., Kageyama, R. and Nishida, E. (2008). FGF induces oscillations of Hes1 expression and Ras/ERK activation. *Curr. Biol.* **18**, R332-R334.
Nikaido, M., Tada, M., Saji, T. and Ueno, N. (1997). Conservation of BMP signaling in zebrafish mesoderm patterning. *Mech. Dev.* **61**, 75-88.
Niwa, Y., Masamizu, Y., Liu, T., Nakayama, R., Deng, C. X. and Kageyama, R. (2007). The initiation and propagation of Hes7 oscillation are cooperatively regulated by Fgf and notch signaling in the somite segmentation clock. *Dev. Cell* **13**, 298-304.
Oates, A. C. and Ho, R. K. (2002). Hairy/E(spl)-related (Her) genes are central components of the segmentation oscillator and display redundancy with the Delta/Notch signaling pathway in the formation of anterior segmental boundaries in the zebrafish. *Development* **129**, 2929-2946.
Palmeirim, I., Henrique, D., IshHorowicz, D. and Pourquie, O. (1997). Avian hairy gene expression identifies a molecular clock linked to vertebrate segmentation and somitogenesis. *Cell* **91**, 639-648.
Pourquie, O. (2003). The segmentation clock: converting embryonic time into spatial pattern. *Science* **301**, 328-330.
Riedel-Kruse, I. H., Muller, C. and Oates, A. C. (2007). Synchrony dynamics during initiation, failure, and rescue of the segmentation clock. *Science* **317**, 1911-1915.
Saga, Y. and Takeda, H. (2001). The making of the somite: molecular events in vertebrate segmentation. *Nat. Rev. Genet.* **2**, 835-845.
Sawada, A., Fritz, A., Jiang, Y. J., Yamamoto, A., Yamasu, K., Kuroiwa, A., Saga, Y. and Takeda, H. (2000). Zebrafish Mesp family genes, mesp-a and mesp-b are segmentally expressed in the presomitic mesoderm, and Mesp-b confers the anterior identity to the developing somites. *Development* **127**, 1691-1702.
Sawada, A., Shinya, M., Jiang, Y. J., Kawakami, A., Kuroiwa, A. and Takeda, H. (2001). Fgf/MAPK signalling is a crucial positional cue in somite boundary formation. *Development* **128**, 4873-4880.
Scholpp, S. and Brand, M. (2004). Endocytosis controls spreading and effective signaling range of Fgf8 protein. *Curr. Biol.* **14**, 1834-1841.
Uriu, K., Morishita, Y. and Iwasa, Y. (2009). Traveling wave formation in vertebrate segmentation. *J. Theor. Biol.* **257**, 385-396.
Wahl, M. B., Deng, C., Lewandoski, M. and Pourquie, O. (2007). FGF signaling acts upstream of the NOTCH and WNT signaling pathways to control segmentation clock oscillations in mouse somitogenesis. *Development* **134**, 4033-4041.
Warga, R. M. and Kimmel, C. B. (1990). Cell movements during epiboly and gastrulation in zebrafish. *Development* **108**, 569-580.